European Polymer Journal 46 (2010) 1896–1907

Contents lists available at ScienceDirect

European Polymer Journal

journal homepage: www.elsevier.com/locate/europolj

Relevance of the femtolaser notch sharpening to the fracture of ethylene–propylene block copolymers

A. Salazar [a,*], J. Rodríguez [a], A. Segovia [b], A.B. Martínez [b]

[a] Departamento de Ciencia e Ingeniería de Materiales, Escuela Superior de Ciencias Experimentales y Tecnología, Universidad Rey Juan Carlos, C/ Tulipán s/n, 28933 Móstoles, Madrid, Spain
[b] Centre Català del Plàstic – Universitat Politècnica de Catalunya, C/ Colom 144, 08222 Terrassa, Barcelona, Spain

ARTICLE INFO

Article history:
Received 22 December 2009
Received in revised form 12 May 2010
Accepted 28 June 2010
Available online 30 June 2010

Keywords:
Femtolaser sharpening
Razor sharpening
Fracture toughness
Ethylene–propylene block copolymer

ABSTRACT

The effect of the notch sharpening on the fracture toughness measured under Linear Elastic Fracture Mechanics (LEFM), Elastic–Plastic Fracture Mechanics (EPFM) and Post-Yielding Fracture Mechanics (PYFM) approaches has been evaluated. Bulk and film specimens of an ethylene–propylene block copolymer have been analyzed. The samples for fracture characterization were sharpened using a steel razor blade and the femtosecond laser ablation technique. Both notching techniques give rise to crack tip radii of the very same size. The fracture toughness of the specimens sharpened via femtolaser were ~10%, ~75% and ~90% lower than that of the specimens sharpened via razor blade when determined with the help of LEFM, the EPFM approach as the multiple specimen method, and by the Essential Work of Fracture, respectively. Both in the bulk samples as in the films, the presence of plastic deformation, either large or small, occurring ahead of the crack tip during the sharpening seems to be the reason for the difference in the fracture values.

1. Introduction

The evaluation of the fracture toughness either in bulk or polymer films requires that the body contains a sharp crack with a radius lesser than 20 μm, according to ESIS (European Structural Integrity Society) [1–3] and ASTM (American Society for Testing and Materials) [4–6] guidelines. The quality of the notch is of deciding importance to determine well established *J–R* resistance curves or Essential Work of Fracture (EWF) parameters in bulk and polymer films, respectively, and therefore, critically dependent on the notch sharpening technique.

Previous works have shown that the notch sharpening procedure is crucial when evaluating the fracture toughness. Martínez et al. [7] analyzed the fracture toughness of an ethylene–propylene block copolymer film with the help of the EWF methodology [3]; meanwhile Salazar et al. [8] studied the fracture toughness of a bulk ethylene–propylene block copolymer at different temperatures and strain rates with the aim of ensuring Linear Elastic Fracture Mechanics (LEFM) and Elastic–Plastic Fracture Mechanics (EPFM) conditions. In both cases, the sharpening of the specimens was performed using steel razor blades and a femtosecond pulsed laser. The femtosecond pulsed laser ablation is characterized by very rapid creation of vapor and plasma phases, negligible heat conduction and the absence of a liquid phase [9,10]. Thus, this technique can remove the material of the notch tip by ablating it with almost no heat dissipation, preventing melting and thermal deformations of the surrounding area. These works proved that, independently of the fracture mechanics conditions, the fracture toughness of the specimens sharpened through femtosecond laser ablation showed lower values compared to those obtained in the samples sharpened using a steel razor blade. The damage produced ahead of the crack tip through plastic deformation in the steel razor blade sharpened samples is the reason of this increase in the fracture toughness.

* Corresponding author. Fax: +34 914888150.
E-mail address: alicia.salazar@urjc.es (A. Salazar).

0014-3057/$ - see front matter © 2010 Elsevier Ltd. All rights reserved.
doi:10.1016/j.eurpolymj.2010.06.012

The conclusions drawn from the investigations performed by Martínez et al. [7] and Salazar et al. [8] indicate not only that the sharpening method influences significantly the fracture parameters of ethylene–propylene block copolymers, but also that these differences were more noticeable under elastic–plastic and fully plastic conditions, reaching up to ~25% and ~50%, respectively.

In the light of these previous results, the aim of the present work is to investigate more deeply and systematically the influence of the notch sharpening on the fracture parameters of ethylene–propylene block copolymers. For that, the very same material was tested under very diverse conditions using different geometries, from thin films to much thicker specimens. The LEFM, EPFM and Post-Yielding Fracture Mechanics (PYFM) were used to analyze the experimental data in each case, comparing the results achieved with the traditional sharpening using steel razor blades and those obtained after notch sharpening with a femtosecond pulsed laser.

2. Theoretical background

At high loading rates and room temperature, the load (P)–displacement (δ) diagrams of bulk ethylene–propylene block copolymers show a linear response and the LEFM assumptions are fulfilled, so the basic guidelines of ESIS TC4 Protocol "Determination of fracture toughness (G_{IC} and K_{IC}) at moderately high loading rates" were followed [11]. However, at low loading rate and room temperature, the P–δ records present a pronounced non-linearity brought about by contained plastic deformation. Fracture characterization is achieved with the help of the EPFM multiple specimen methodology, which allows the construction of the J–R curve through a set of nominally identical specimens loaded to different displacements to get distinct amounts of stable crack growth, Δa. In such a case, the basic guidelines of ESIS TC4 Protocol "J-fracture toughness of polymers at slow speed" are applied [2].

On the other hand, the mechanical response of polymer films is governed by the fully yielded situation which occurs in the plane stress fracture state. This behaviour entails the usage of the PYFM approach such as the EWF theory for the evaluation of fracture parameters. The instructions given by the ESIS TC4 Protocol "Essential Work of Fracture" were taken as a guide [3]. A brief description of the methods utilized is now presented.

2.1. The LEFM method

At impact conditions, the LEFM assumptions are met, so fracture toughness, K_{IC}, can be calculated with [1]

$$K_{IC} = f\frac{P}{BW^{1/2}} \tag{1}$$

where B is the thickness, W is the width and f is a geometrical factor that can be computed using the expression

$$f = 6\alpha^{1/2} \times \frac{[1.99 - \alpha(1-\alpha)(2.15 - 3.93\alpha + 2.7\alpha^2)]}{(1+2\alpha)(1-\alpha)^{3/2}} \quad \text{for SENB} \tag{2}$$

being $\alpha = a_o/W$. Since the geometrical factor f is a function of the initial crack length, a_o, the determination of the fracture toughness was made using a series of test specimens with equal dimensions but varying initial crack lengths. K_{IC} values were obtained from the plot load of fracture initiation, P, versus $BW^{1/2}/f$. These data should best fit a straight line which slope is the fracture toughness. The load at fracture initiation was estimated following the guidelines of ESIS procedures [1,11].

Values of K_{IC} under plane strain are valid if the following criteria are achieved:

$$B, a, W - a > 2.5\left(\frac{K_{IC}}{\sigma_Y}\right)^2 \tag{3}$$

where σ_Y is the yield stress of the material.

2.2. The EPFM multiple specimen method

To determine the initiation toughness parameter under elastic–plastic conditions, J_{IC}, the J–R curve is to be constructed, where J is plotted versus the ductile crack extension, Δa. The multiple specimen method, first proposed by Landes and Begley [12], is the most common approach for deducing J–R curves. A set of identical specimens is loaded to various displacements, unloaded, cooled at low temperatures and finally fractured. The initial and final stable crack lengths are measured physically from the broken surfaces [2], while J is calculated from the total energy required to extend the crack, U, which is determined from the area under the load versus load-point displacement curve up to the line of constant displacement corresponding to the termination of the test:

$$J = \frac{2U}{B(W - a_0)}. \tag{4}$$

The resulting J-crack growth resistance curve should be described by a power law $J = C \cdot \Delta a^N$, with $N \leqslant 1$. The crack initiation resistance, J_{IC}, is a difficult parameter to determine when blunting and notch deformation by yielding occur, being these plastic phenomena strongly dependent on the notch sharpening technique. Thus, the notch sharpening procedure is of major importance for J_{IC} values.

For the computation of J_{IC} values, the guidelines described by Hale and Ramsteiner [2] have been followed, where this critical value has been replaced by a pseudo-initiation value $J_{0.2}$, which defines crack resistance at 0.2 mm of the total crack growth.

The size requirements for plane strain J_{IC} are given by [13]:

$$B, a, W - a > 25\frac{J}{\sigma_Y} \tag{5}$$

2.3. The EWF method

The EWF method was firstly proposed by Cotterell and Reddel [14], who developed Broberg's idea about the stable crack growth [15]. This procedure is based on the hypothesis that the total energy involved during the ductile fracture (i.e. plastic deformation fully developed around the

ligament region prior to the crack growth) of a precracked specimen, W_f, can be divided into two terms,

$$W_f = W_e + W_p \tag{6}$$

where W_e is called the "essential work of fracture" and represents the energy involved in the creation of two new surfaces during the crack propagation. This energy is associated with the fracture process zone (FPZ) (Fig. 1), as it is the region where the real fracture process takes place with the formation of two new surfaces. The second term, W_p, is called the plastic work or the "non-essential work of fracture" and collects all other sources of energy dissipated during the fracture, such as plastic deformation and other dissipative processes. This energy is related to the outer area of the fracture process zone (Fig. 1), also named the outer plastic zone (OPZ).

The essential work involves the creation of new surfaces and is proportional to the area of the FPZ with a ligament length, l, while the plastic work is proportional to the volume of the OPZ. These concepts allow us to rewrite Eq. (6) in the following manner:

$$W_f = w_e \cdot l \cdot t + \beta \cdot w_p \cdot l^2 \cdot t \tag{7}$$

where t is the sheet thickness and β is the plastic zone shape factor. Normalizing by the ligament cross-section, $l \cdot t$, the specific work of fracture, w_f, is obtained as a linear function of the ligament length:

$$w_f = w_e + \beta \cdot w_p \cdot l \tag{8}$$

And w_e and $\beta \cdot w_p$ can be derived from the best fit linear regression of data resulting from a series of broken specimens plotted in a diagram of specific total fracture energy against ligament length.

According to EWF protocol [3], some restrictions on the ligament range must be considered:

$$\max(3 \cdot t, 5\ \text{mm}) < l < \min\left(\frac{W}{3}, 2 \cdot r_p\right) \tag{9}$$

where W is the width of the Double Edge Notched Tension (DENT) specimen (recommended by EWF protocol [3] due to consistency and reproducibility) and r_p is the plastic radius defined as:

$$2 \cdot r_p = \frac{\pi}{8} \cdot \frac{E \cdot w_e}{\sigma_Y^2} \tag{10}$$

being E the Young's modulus (E and σ_Y are obtained for the same material in tensile tests and similar testing conditions).

The upper limit of Eq. (9) is intended to avoid edge effects on the fracture, while the lower limit is to guarantee that all the samples are under truly plane stress. The plane stress state of tension of the samples can be checked using the Hill's analysis [16], which consists in the evaluation of the nett cross-section stress, σ_{max}, of the specimens at the maximum load and comparing it with the theoretical maximum value that should be obtained under plane stress conditions given by:

$$\sigma_{max} = 1.15 \cdot \sigma_Y \tag{11}$$

DENT specimens with values of σ_{max} above this limit are not under plane stress conditions according to Hill's assumptions, thus indicating that the development of the plastic zone is restricted. Additionally, the stress values must verify a stress criterion to guarantee that all data are under plane stress and no mixed stress state occurs at any case. The criterion is to reject any essential work data for which the maximum stress is greater than $1.1 \cdot \sigma_m$ or less than $0.9 \cdot \sigma_m$, where σ_m denotes the average value of the maximum stresses of all the tested specimens, σ_{max} [3].

Apart from the ligament full yielding prior to crack propagation, other requisites are to be accomplished to apply properly the EWF method as that the crack propagation must be steady and there must be a common fracture phenomenology in all ligament lengths, visible in the self similarity of the curves in the load–displacement records.

The specific essential work of fracture, w_e, is regarded as a material constant dependent only on thickness and equivalent to J_{IC} [17], which has been also supported experimentally by different authors [18–20] and compared with the CTOD values [21,22]. However, the EWF method compared to the J-integral procedure presents some advantages as its simplicity and applicability to thinner specimens.

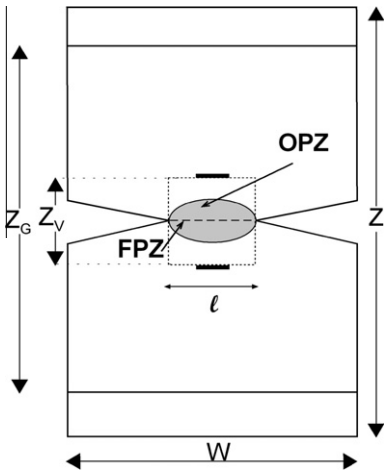

Fig. 1. DENT specimen showing the typical dimensions and the location of the FPZ and OPZ.

3. Experimental procedure

3.1. Materials

The material studied was a commercial grade ethylene–propylene block copolymer, EPBC, supplied by Repsol in form of pellets. The bulk specimens for fracture characterization were prepared by injection moulding meanwhile cast-extruded films with a nominal thickness of 1 mm were utilized.

The basic characteristics such as the ethylene content and the isotactic index determined from Nuclear Magnetic Resonance (NMR), the glass transition temperatures corresponding to the elastomeric particles, T_g EPR, embedded in the propylene matrix, T_g PP, measured via Dynamic

Mechanical Thermal Analysis (DMTA) and molecular weights obtained by Gel Permeation Chromatography (GPC) are collected in Table 1.

The mechanical properties such as the Young's modulus, E, and the yield stress, σ_Y, were measured via tensile tests at cross-head speeds of 1 mm/min for the ISO-527 bulk injected tensile samples and 2 mm/min for the extruded polymer films. The sheets were mechanically characterized along the Machine Direction (MD). The results are gathered in Table 2. Elastic modulus is governed by the cooling rates during the manufacture of the polymers, affecting the resulting crystallinity degree [23]. The differences in the processing of bulk specimens and films justify the results collected in Table 2.

3.2. Sample preparation

Fracture toughness tests on bulk specimens were carried out on injected single edge notched bend specimens (SENB) with 6.35 and 9 mm thick, being the overall dimensions of $6.35 \times 12.7 \times 55$ and $9 \times 18 \times 80$ mm, respectively. In all the specimens, an initial straight-through slot with a length to width ratio of 0.5 and terminating in a V-notch with 0.2 mm in root radius was mechanized.

On the other hand, from the extruded films, DENT specimens as shown in Fig. 1 were cut. The dimensions of the sheets were the following: $W = 60$ mm, $Z = 90$ mm and $Z_G = 60$ mm. Ligament lengths for the DENT samples ranged from 5 to 20 mm. These values were measured on all the specimens before and after the fracture tests, using a profile projector (Starret Sigma VB 300), with a precision on the measurements of ±1 μm. The thickness of the ligament area of the films was determined as the average of three measurements using a micrometer with a precision of ±1 μm.

Two different procedures for the sharpening of either the SENB specimens or the films were carried out:

3.2.1. S-Type

It consists on tapping a fresh steel razor blade into the root of the V-notch (following the ESIS [2] and ASTM [6] guidelines) on the bulk samples and notch pushing using a fresh razor blade on the thin sheets.

3.2.2. F-Type

The sharpening of the notch is produced through femtosecond pulsed laser ablation (Femtolaser) [9,10], using a commercial Ti:sapphire oscillator (Tsunami, Spectra Physics) plus a regenerative amplifier system (Spitfire, Spectra Physics) based on chirped pulse amplification (CPA) technique. 120-fs pulses at 795 nm with a repetition rate of 1 kHz were produced. The scanning speed was 130 μm/s. Eight passes were conducted with a pulse energy of 0.07 mJ. The sharp length inserted by the femtolaser was of 500 μm.

Also, it is worth mentioning that alternative sharpening procedures such as blade tapping on cooled specimens were explored with no success to achieve an acceptable natural crack.

The total initial crack depth, a_o, to width ratio after sharpening for the bulk specimens utilized for fracture characterization was of 0.55.

The morphology and dimensions of the crack tip after sharpening and the area beneath it of the non-tested specimens were analyzed via light microscopy (Leica DMR) and scanning electron microscopy (JEOL JSM-5610). Concerning the bulk samples, a previous preparation was to be made consisting on sectioning the bulk copolymer into films with thickness in the range between 6 and 10 μm with the help of a microtome (Rotary Microtome Leica RM2265). The resulting sections were picked up and mounted on microscope slides to be analyzed via transmitted light microscopy.

3.3. Fracture tests

3.3.1. Fracture characterization of bulk specimens at high strain rate

In order to guarantee the applicability of LEFM approach, fracture toughness tests at high strain rates were carried out on an instrumented Charpy impact pendulum (Ceast), basically following the guidelines described by ESIS TC4 Protocol for "the determination of fracture toughness at moderately high loading rates" [11]. All the materials with a thickness of 9 mm were tested at room temperature using a three-point bend fixture with a span to width ratio of 4. At least, six specimens with a total initial crack length varying over the range $0.3 \leqslant a/W \leqslant 0.65$ were tested to obtain K_{IC}. This procedure was preferable instead of using the data of five replicates (same crack length) to reduce the statistical variance. The initial velocity was of 1.25 m/s and this condition was accomplished with an equivalent striker mass of 3.664 kg. Mechanical damping by means of soft pads placed where the striker hits the specimen was used to minimize the dynamic effects.

3.3.2. Fracture characterization of bulk specimens at low strain rate

The ESIS TC4 Protocol entitled "the determination of J-fracture toughness of polymers at slow speed" [2], was followed to achieve the J–R curves from multiple specimens. A minimum of seven samples was tested using an electromechanical testing machine (MTS Alliance RF/100) with a load cell of ±5 kN. The tests were performed at room temperature and under displacement control at a cross-head speed of 1 mm/min using a three-point bend fixture of 50.8 and 72 mm loading spans for the SENB specimens with 6.35 and 9 mm in thickness, respectively.

3.3.3. Fracture characterization of polymer films

To characterize the extruded and injected copolymer films, 20 DENT specimens with ligament lengths varying between 5 and 20 mm were tested at 23 °C. The tests were carried out on a universal testing machine (SUN2500, Galdabini) equipped with a load cell of ±1 kN at a constant cross-head speed 2 mm/min. The procedure described by Gamez-Pérez et al. [24] was followed to obtain the deformation traces: two extensometer marks were drawn on the samples separated by a distance Z_v, equal to the

Table 1
Basic properties of the copolymer under study.

	NMR		DMTA		GPC			
	Ethylene content (%wt)	Isotactic index (%)	T_g PP (°C)	T_g EPR (°C)	M_w (kg/mol)	M_n (kg/mol)	M_z (kg/mol)	Polydispersity (M_w/M_n)
Copolymer	8.5	85.4	10.4	−49.3	353	66	1026	5.37

Table 2
Mechanical properties of thin sheets and bulk specimens of the ethylene–propylene block copolymer.

	E (GPa)	σ_Y (MPa)
Bulk specimens	1.54 ± 0.03	23.9 ± 0.5
Thin sheets	0.93 ± 0.03	20.1 ± 0.2

nominal ligament length of each specimen, l (Fig. 1). The displacement between the extensometer marks, δ, during loading was measured with a videoextensometer (Mintron OS-65D CCD video camera in conjunction with Messphysik software).

The total energy to failure, W_f, was calculated for each specimen as the area under the P–δ curve. The fracture parameters of the copolymer films were computed from the best linear fit of the specific fracture energies against the ligament lengths (w_f versus l).

4. Results and discussion

4.1. Fracture characterization of bulk copolymers at high strain rate – LEFM approach

Fig. 2a and b show the load–time curves recorded from impact tests for razor blade (S-Type) and femtolaser (F-Type) sharpened specimens, respectively. Six impact tests were performed for each type of sharpened specimen resulting from varying the initial crack length to width ratio from 0.3 to 0.65. In relation to the inertial effects, S-Type impact tests were carried out firstly. Although soft pads were utilized to reduce inertial effects, load oscillations were evident in Fig. 2a. However, the amplitude load is confined to the allowed limits for polymer impact testing. In case of F-Type impact tests, it was decided to increase the thickness of the soft pads and consequently, the resulting graphs were smoother (Fig. 2b).

The fracture toughness values, K_{IC}, were obtained from the slope of a straight line fit of the diagrams of load at fracture initiation, P, versus $BW^{1/2}/f$. These curves for S-Type and F-Type sharpened specimens, together with their corresponding fracture toughness values, are plotted in Fig. 3. Under these testing conditions, the fracture toughness of S-Type specimens, 3.10 ± 0.04 MPa $m^{1/2}$, is slightly higher than that of F-Type specimens, 2.80 ± 0.06 MPa $m^{1/2}$. With the aim of checking the size criteria (Eq. (3)), the yield stress at 23 °C and impact strain rates should be used (roughly five orders of magnitude higher than quasi-static strain rates). Gómez del Río et al. [25] have studied the strain rate and temperature influence on the tensile yield stress in this very

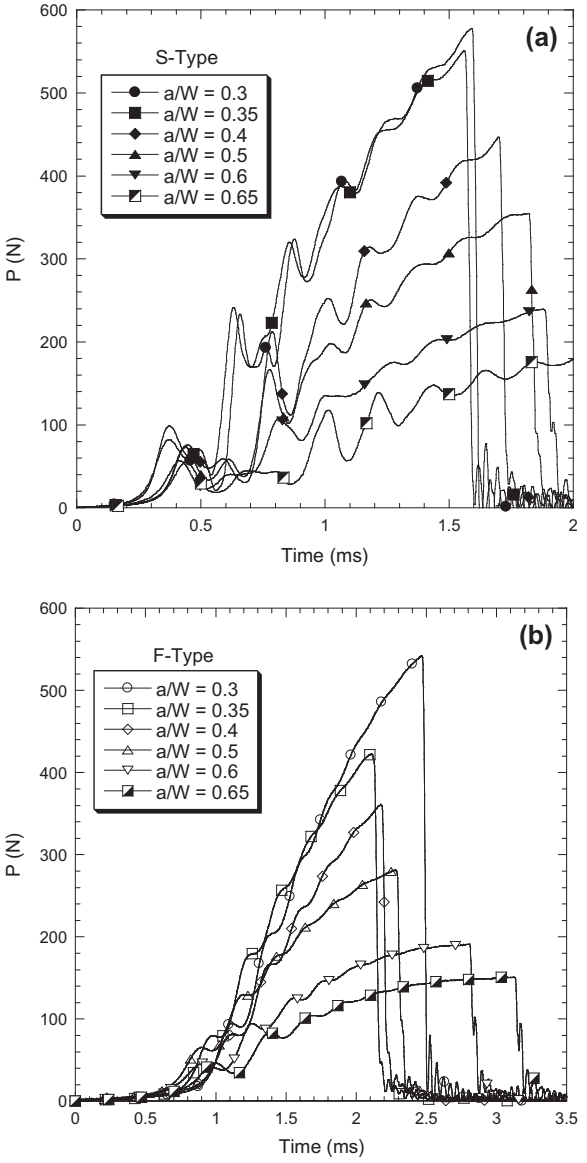

Fig. 2. Load–time records obtained from impact tests for (a) S-Type and (b) F-Type specimens.

copolymer. From this work, an impact yield stress estimation of ~55 MPa has been obtained and the corresponding K_{IC} values were in plane strain as Eq. (3) was fulfilled.

The differences between the K_{IC} values of the S-Type and F-Type samples are utmost of 11% and can be accounted for

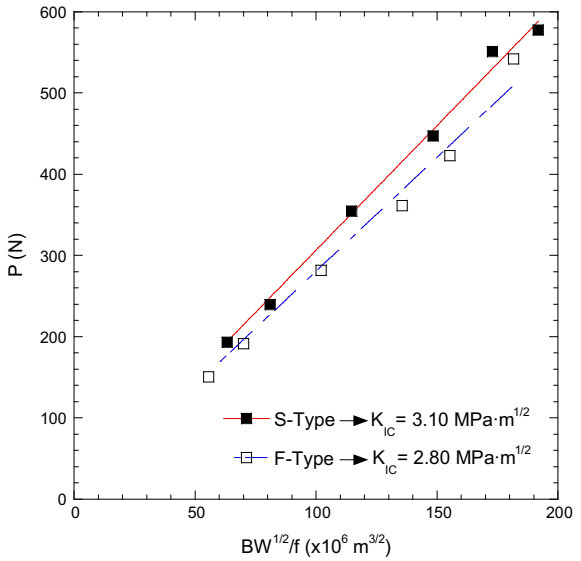

Fig. 3. Determination of K_{IC} at high loading rates for S-Type and F-Type specimens from the slope of the curves load at fracture initiation, P, versus $BW^{1/2}/f$.

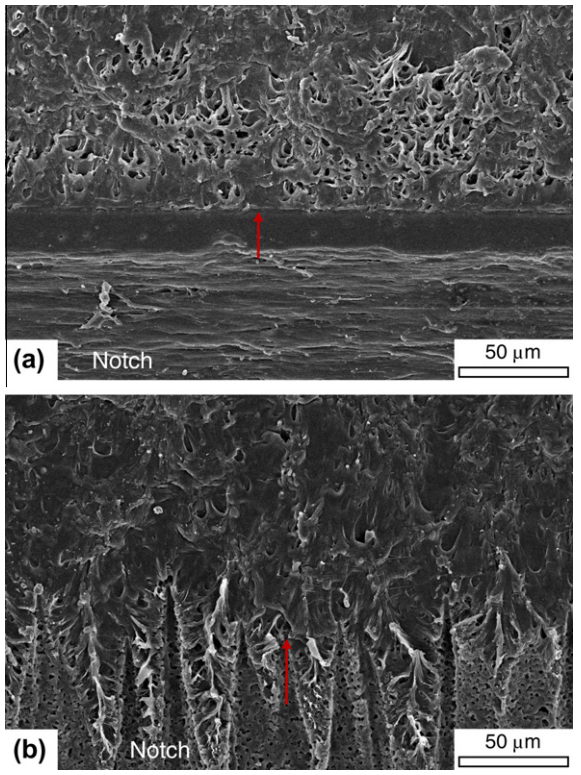

Fig. 4. Fracture surfaces obtained from the broken specimens tested at high loading rate of (a) S-Type and (b) F-Type sharpened samples. The arrow delimitates the notch from the fracture surface.

by the examination of the fracture surfaces of the distinct sharpened specimens (Fig. 4). The fracture surface ahead of the notch tip of the S-Type samples (Fig. 4a) presented evi-

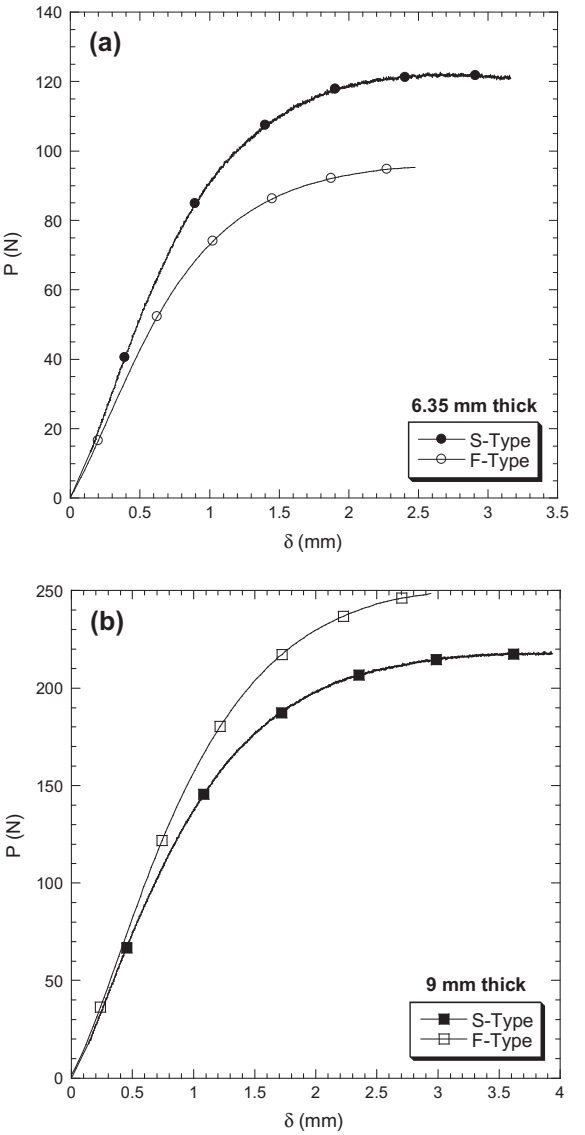

Fig. 5. Load (P) versus displacement (δ) of S-type and F-Type samples with (a) 6.35 mm and (b) 9 mm in thickness.

dent traces of plastic deformation in the form of ductile tearing of the PP matrix. On the contrary, the fracture surface close to the notch tip in the F-Type samples (Fig. 4b) presented a brittle appearance with no signs of ductility all along the depth of the bulk specimen. Besides, in this figure it can be appreciated the traces of the femtosecond laser ablation pulses at the crack tip. Hence, the plastic deformation caused during the sharpening seems to be the main factor affecting the fracture toughness in bulks specimens tested at high strain rates [7,8].

4.2. Fracture characterization of bulk copolymers at low strain rate – EPFM approach

Fig. 5a and b show the load versus load-line displacement curves associated with the S-Type and F-Type sharp-

ened specimens with 6.35 and 9 mm in thickness, respectively. As can be seen, the mechanical response is highly non-linear and the multiple specimen method is applied to determine the J-crack growth resistance curves. The difference in stiffness is due to different lengths of the initial cracks.

Fig. 6a and b combine the *R*-curves of the S-Type and F-Type specimens with 6.35 and 9 mm thick, respectively. These plots also include the fit of the J-crack growth resistance curve to the power law $J = C \cdot \Delta a^N$, with $N \leqslant 1$. Independently of the specimen's dimensions, the resistance curve of F-Type is below the one of S-Type. This tendency was also observed by Salazar et al. [8] in another copolymer similar to the one under study in the present work except for slight differences in the molecular weight. On the other hand, according to the fittings, for the same procedure of notch sharpening, there seems to be no great influence of the thickness on the resistance curves.

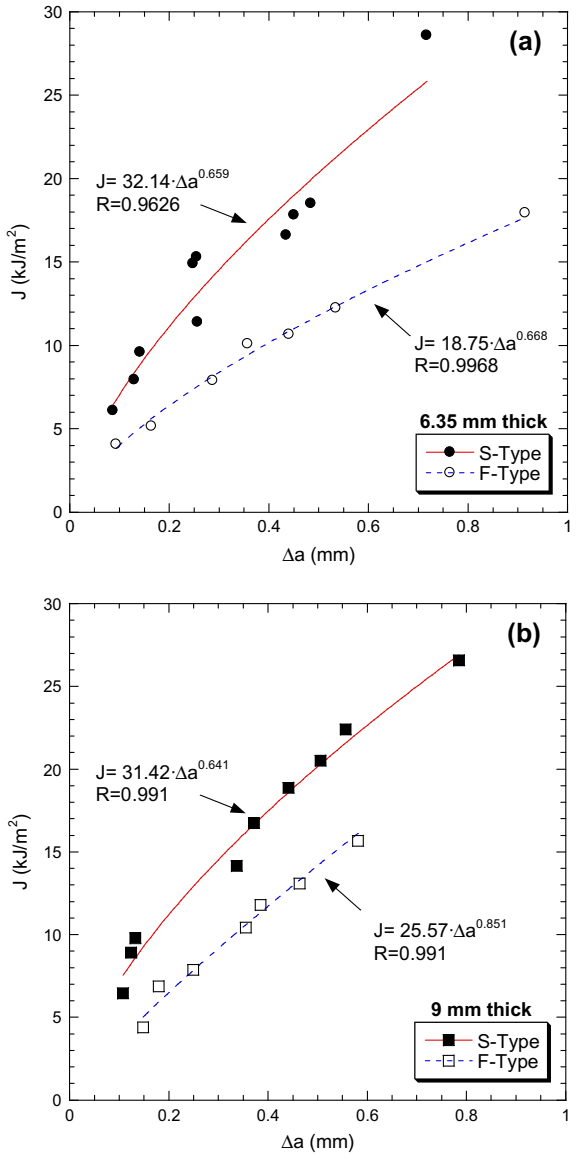

Fig. 6. *J–R* curves for S-Type and F-Type specimens determined from (a) 6.35 mm and (b) 9 mm thick samples.

Table 3 collects the fracture toughness, J_{IC}, obtained from the resistance curves of S-Type and F-Type specimens with 6.35 and 9 mm in thickness. Attending to Eq. (5), the values are not in plane strain state except for that related to the F-Type and 9 mm thick specimens, which verify the size requirements. The initiation toughness reflected the influence of the sharpening procedure as the specimens sharpened with a steel razor blade, S-Type, showed in all the cases higher values in the energy for crack growth initiation than the samples sharpened with the femtosecond laser, F-Type. The differences reached up to 74% and 72% for the 6.35 and 9 mm thick specimens, respectively.

Figs. 7 and 8 show micrographs obtained by transmitted light microscopy of microtomed films with ~8 μm thick of the appearance of the crack tip and the area ahead of it of the S-Type and F-Type sharpened specimens with 6.35 and 9 mm thick before being tested, respectively. The crack tip has been marked with an arrow and the measurements carried out at high magnification of the crack tip radius indicated that, independently of the sharpening procedure and dimensions, the values were similar and ranging between 1 and 2 μm. However, there is a dark area in the material facing the crack tip (outlined with dots) which extends deeper in the S-Type samples (Figs. 7a and 8a) than in the F-Type specimens (Figs. 7b and 8b). Besides, in average, it can be observed that the dotted zone of the S-Type 6.35 mm thick specimens (Fig. 7a) was bigger than that of the S-Type 9 mm thick specimens (Fig. 8a). This contrasts with the analysis of the F-Type samples as a function of the thickness (Fig. 8a and b), because this tendency with the thickness could not be observed. According to previous works [7,8], the region ahead of the crack tip with different texture to the rest of the virgin surface is caused during the notch sharpening. During the sharpening procedure with the fresh steel razor blade, the force at the tapping acts along the depth which leads to stresses which exceed the yield stress locally and generate wide plastic deformation areas. The extension of these areas is higher as the depth of the specimens decreases assuming that roughly the same force is applied independently of the thickness of the samples. On the other hand, the dark zone in the F-Type specimens is demonstrated to be related with some incipient lateral removal of material due to the final pulses of the laser ablation process and not with plastic deformation [8].

Consequently, the presence of plastic deformation, either large (6.35 mm thick specimens) or small (9 mm thick specimens), account for the differences in the J_{IC}

Table 3
Fracture toughness values, J_{IC}, of S-Type and F-Type specimens with 6.35 and 9 mm in thickness.

Thickness (mm)	J_{IC} (kJ/m^2)	
	S-Type	F-Type
6.35	11.13	6.40
9	11.20	6.50

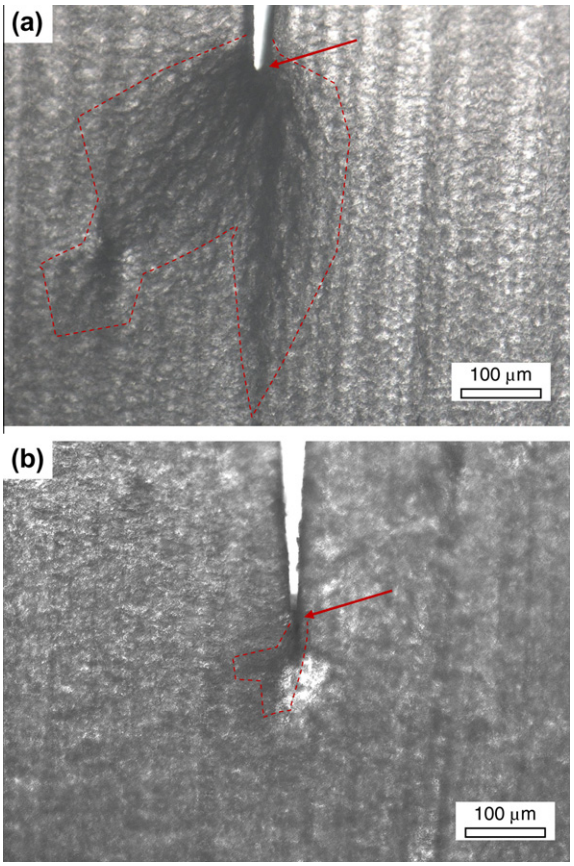

Fig. 7. Micrographs of the crack tip of non-tested (a) S-Type and (b) F-Type sharpened specimens with 6.35 mm in thickness. The arrow points out the end of the crack tip and the damage produced by plastic deformation is outlined by a dotted line.

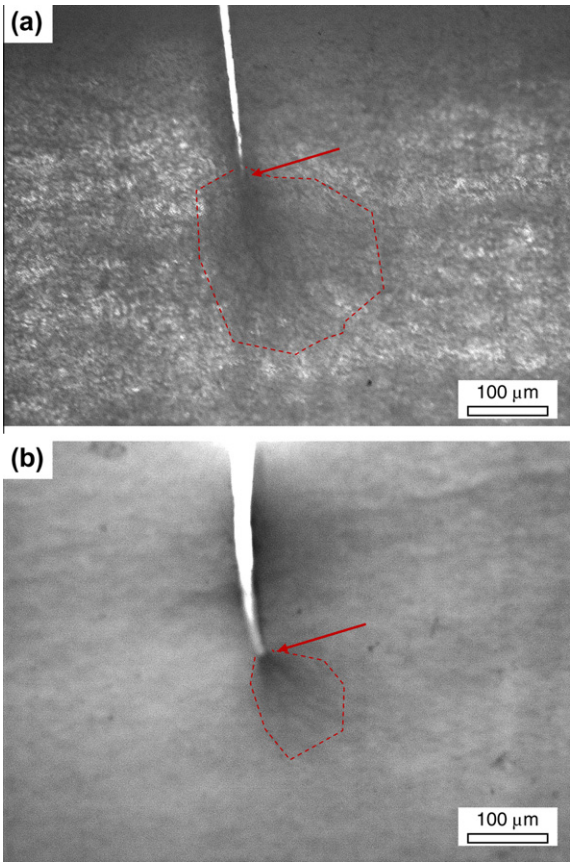

Fig. 8. Micrographs of the crack tip of non-tested (a) S-Type and (b) F-Type sharpened specimens with 9 mm in thickness. The arrow points out the end of the crack tip and the damage produced by plastic deformation is outlined by a dotted line.

values of the distinct sharpened specimens when measured within EPFM regime. The energy necessary to start crack growth is higher when the crack tip encounters a deformed area (S-Type) than when encountering the virgin material (F-Type) because of the different mechanical properties of the crack front matter. Additionally, the analysis of bulk specimens with distinct thickness and different extension of the strain hardened zone ahead of the crack tip in the S-Type samples seems not to affect the quantitative differences of ~75% between distinct sharpened samples. The differences seem to lie in the presence or lack of plastic deformation.

4.3. Fracture characterization of copolymer films – PYFM approach

Fig. 9a and b collect typical P–δ curves at various ligament lengths ranging from ~5 to ~20 mm for S-Type and F-Type cast-extruded copolymer films, respectively. In case of the S-Type, 16 tests were carried out, from which three were to be discarded because they did not fulfil the requisite of the self similarity in the P–δ records (Fig. 9a). On the other side, all the tests performed on the F-Type sharpened films satisfied the geometrical similarity between specimens of different ligament lengths during crack growth (Fig. 9b). Before the determination of the EWF parameters, the stress criterion specified in Section 2.3 was checked to guarantee the plane stress state of tension of all the samples. For that, the maximum net section stresses, σ_{net}, as a function of the ligament lengths are plotted in Fig. 10a and b for S-Type and F-Type extruded films, respectively. In every case, the maximum stress falls in the range defined by the limits $\sigma_m \pm 10\%$, this implies that all the ligaments were grossly yielded as well as the accomplishment of the plane stress state. In addition, these plots revealed that the σ_{net} values of the S-Type samples were similar to the theoretical maximum cross-section stress, σ_{max}, (Eq. (11)). Even higher values were obtained in specimens with shorter ligaments (Fig. 10a). This contrasts with all the F-Type σ_{net} values which were lower than σ_{max} (Eq. (11)) (Fig. 10b). This dissimilarity tendency in the σ_{net} may be attributed to some damage ahead of the crack tip.

From the areas under the P–δ diagrams, the specific work of fracture, w_f, was calculated and plotted against the ligament length, l, for the S-Type and F-Type extruded copolymer films as shown in Fig. 11. The EWF parameters, together with their corresponding standard deviations, are also collected in Table 4. The analysis of the fracture

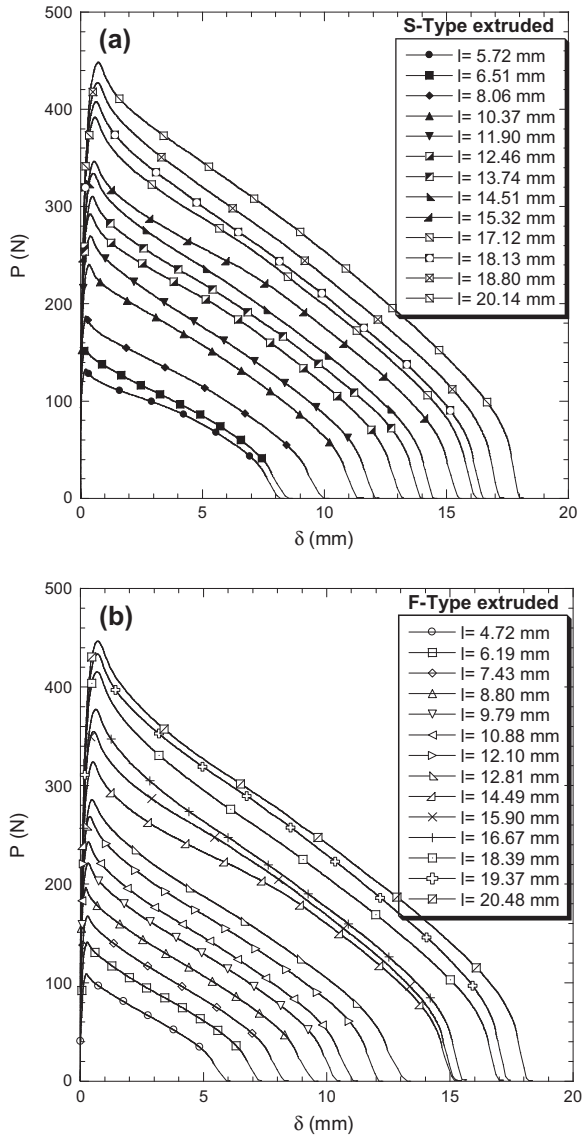

Fig. 9. Load (P)–displacement (δ) traces of cast-extruded DENT copolymer films sharpened via (a) steel razor blade, S-Type, and (b) femtolaser ablation, F-Type.

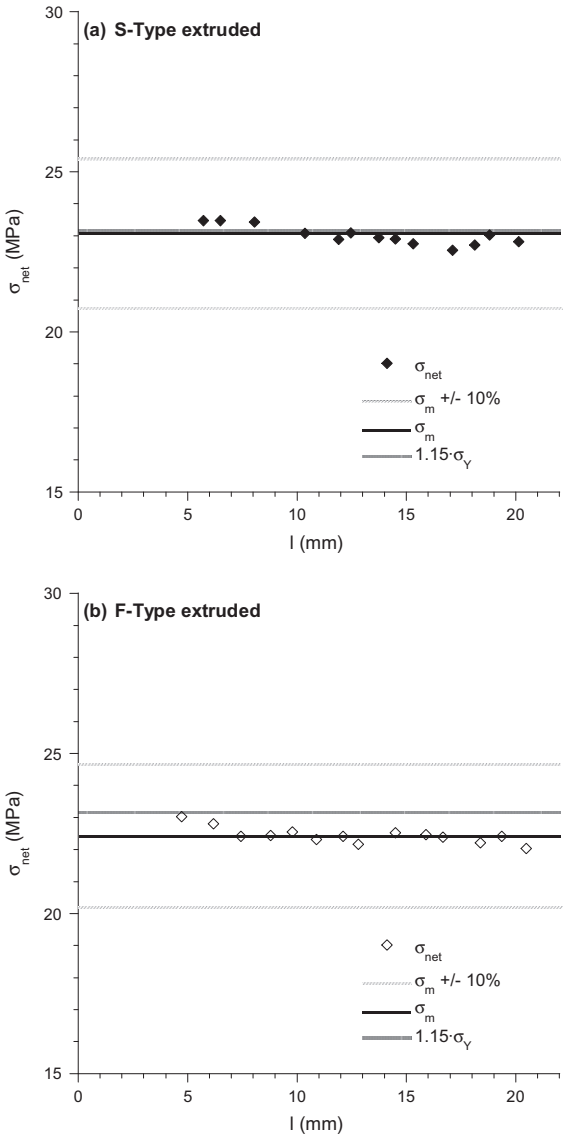

Fig. 10. Stress criterion fulfilment for (a) S-Type and (b) F-Type extruded copolymer films.

parameters of the extruded films reveals that the differences in the essential work of fracture, w_e, are as high as 88%, being the S-Type w_e value almost twice that of the F-Type. Concerning the plastic term defined by $\beta \cdot w_p$, the difference was not so remarkable, the $\beta \cdot w_p$ value of the F-Type sheets was 12% higher than that of the S-Type. These differences can be argued in view of the microscopic examination of the notch quality of the non-tested S-Type and F-Type sharpened films. Fig. 12a and b shows the micrographs obtained via light microscopy of the appearance of the crack tip at the surface of the S-Type and F-Type films, respectively. The crack tip has been marked with an arrow. The observation of the S-Type films revealed a huge and dark area extending ahead of the crack tip (Fig. 12a). This contrast with the analysis of the same region in the F-Type films (Fig. 12b) where not such big damage could be detected. The analysis at high magnification of the crack tip front via scanning electron microscopy (Figs. 13 and 14) allowed us to measure the crack tip radius and visualize the morphology of the damage. The crack tip radius in all cases was lower than 2 μm, so this factor is insignificant for the EWF parameters. In the S-Type films, the crack front presented a different texture to that of the virgin material which showed the presence of plastic deformation (Fig. 13a and b). A closer examination of this area showed that as a consequence of the plastic deformation, some accumulation of material is detected because matter has been dragged during the notch sharpening with the razor blade (Fig. 13c). On the contrary, no signs of plastic deformation ahead of the crack tip in the F-Type could be evidenced except for some incipient lateral removal of

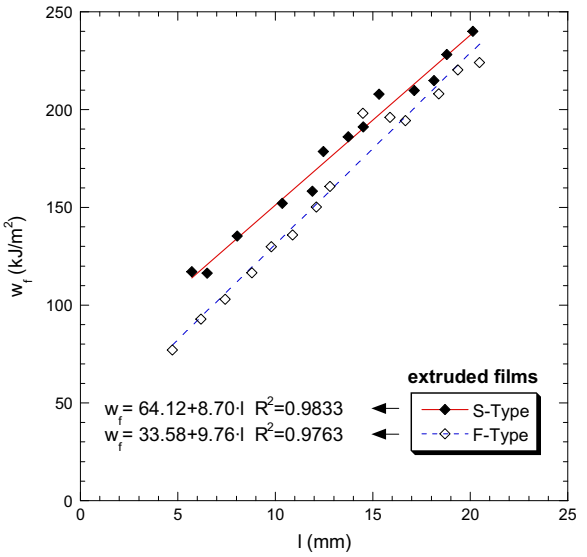

Fig. 11. Linear regression of the specific work of fracture versus ligament length plots for S-Type and F-Type extruded copolymer films for the evaluation of EWF parameters.

Table 4
EWF parameters for S-Type and F-Type extruded films.

Notch sharpening	EWF parameters	
	w_e (kJ/m^2)	$\beta \cdot w_p$ (MJ/m^3)
S-Type	64 ± 5	8.7 ± 0.3
F-Type	34 ± 6	9.8 ± 0.4

material due to the final pulses of the laser ablation process at the very surface (Fig. 14).

Under fully plastic conditions, the differences found in the w_e values reach up to ~90% between the razor blade and femtolaser sharpening films. As in the case of the bulk specimens, the reason of such large disparity is the presence or lack of plastic deformation ahead of the crack tip. The essential work of fracture, w_e, represents the energy necessary to yield the ligament area in the process zone and to start the crack growth. This energy is higher in films with an already deformed area, as is the case of the razor blade sharpened films, than in the case of a non-deformed area like the femtolaser sharpened films. The material facing the crack tip in the S-Type films is strain hardened and their mechanical properties are different to that of the virgin material in the F-Type thin sheets. On the other hand, the plastic term, $\beta \cdot w_p$, which is related to the energy dissipated in the outer process zone, hardly is affected by the sharpening procedure. Then, the sharpening method only affects the essential work of fracture, w_e.

4.4. Influence of the notch sharpening

The different influence of the notch sharpening on the results obtained from specimens tested under LEFM, EPFM or PYFM conditions is striking. As it has been previously shown, the fracture toughness values of the femtolaser

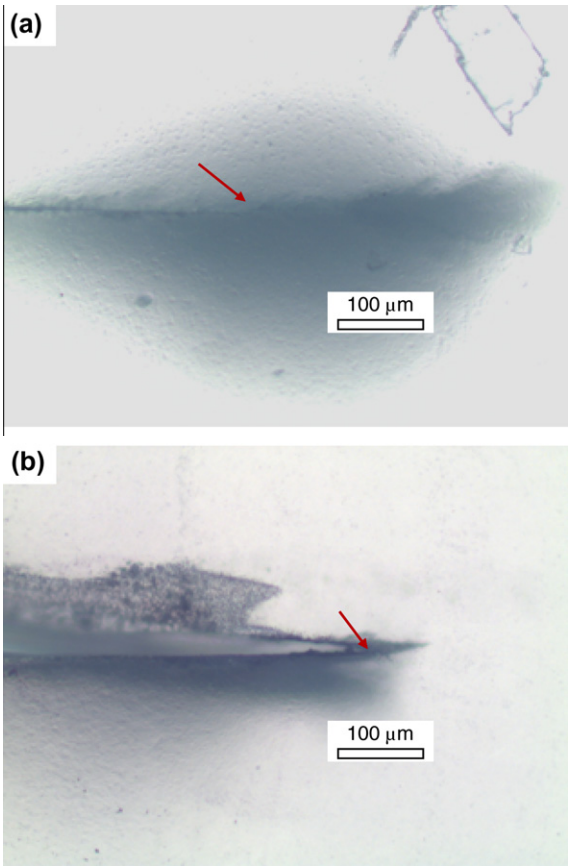

Fig. 12. Light micrographs of the crack tip of non-tested extruded (a) S-Type and (b) F-Type sharpened films. The arrows point out the end of the crack tip.

sharpened specimens are always lower: 11%, 75% and 90% when the specimens are tested under conditions of LEFM, EPFM or PYFM, respectively. The application of the plane strain criteria leads to different conclusions: the specimens tested following LEFM are always under a plane strain state; when the testing is performed under EPFM approach some specimens are in a plane strain state but others do not, indicating a transitional behaviour; finally, all the specimens tested according to the PYFM methodology are in a full plane stress state. There seems to be a relationship between the stress state and the influence of the notch sharpening technique. This is logical taken into account the plastic deformation produced during the crack generation by forcing the razor blade into the notch root. The ratio between plastic zone size and specimen thickness is much associated with the stress state. Experiments show that the closer the stress state to plane strain conditions the lower effect of notch sharpening technique. More research is needed to extend this conclusion to other materials different from the ethylene–propylene block copolymers.

One of the basis and driving forces of fracture testing is the similitude argument: any crack in any body of the same material will fracture under the same value of fracture parameters such as the stress intensity factor or the

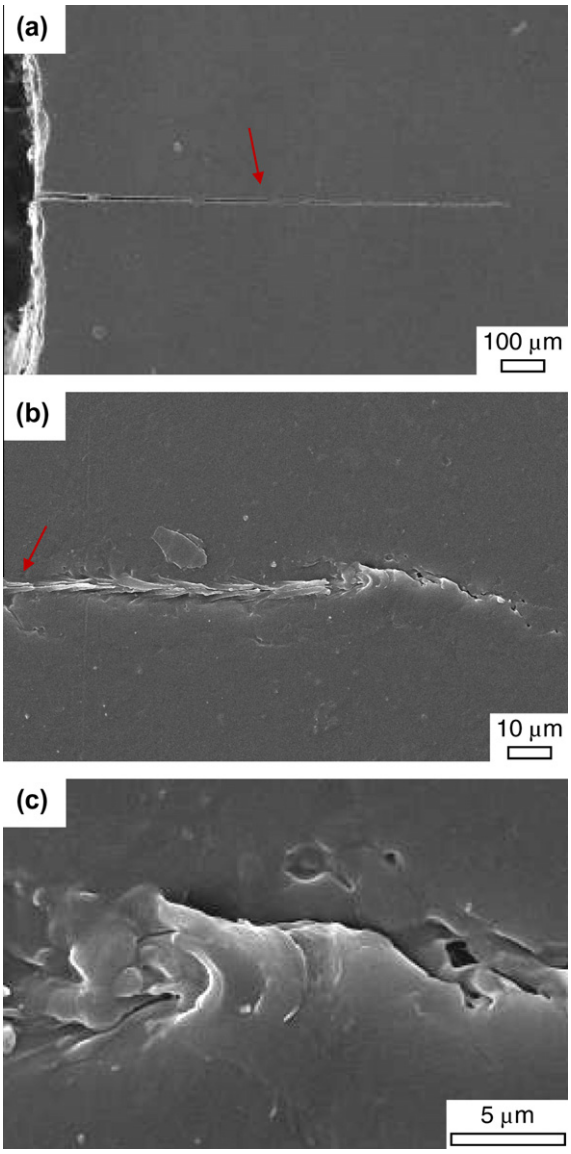

Fig. 13. Micrographs of the crack tip of the non-tested extruded S-Type sharpened films obtained via scanning electron microscopy: (a) sharpened region, (b) detail of the crack tip front and (c) damage ahead of the crack tip. The arrows point out the end of the crack tip.

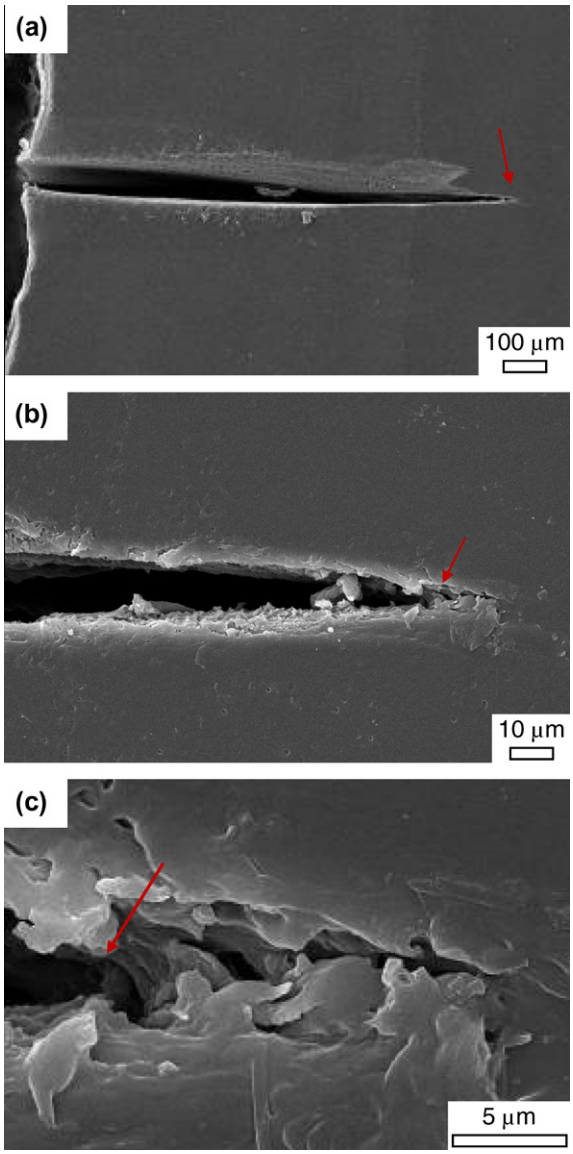

Fig. 14. Micrographs of the crack tip of the non-tested extruded F-Type sharpened films obtained via scanning electron microscopy: (a) sharpened region, (b) detail of the crack tip front and (c) damage ahead of the crack tip. The arrows point out the end of the crack tip.

J-integral. Specimen preparation has been recognized as critical in standards and protocols developed by the integrity societies like ASTM or ESIS. In metals, the crack is grown from a normalized starter notch by fatigue under controlled conditions, but cracks in polymers cannot be easily achieved by this method and the use of the razor blade has been chosen as an alternative.

The fact that the specimens sharpened through femtosecond laser ablation provide systematically lower fracture toughness values than those sharpened by the traditional steel razor blade questions the validity of the similitude concept. How can two specimens be compared if different plastic zones are developed ahead of the crack before the loading is applied? This is a crucial aspect that should be considered in any standardization effort in the field of fracture testing of polymers. Unfortunately, the elevated cost of the femtolaser notching makes at present the introduction of this procedure in a fracture standard inaccessible and more research is necessary before this technique can be used in a standard.

5. Conclusions

The influence of the notch sharpening on the fracture toughness obtained under LEFM, EPFM and PYFM conditions has been evaluated in an ethylene–propylene block copolymer. Independently of the fracture mechanics

approaches, the fracture toughness of the specimens sharpened through femtosecond laser ablation showed lower values compared to those measured on samples sharpened using a steel razor blade. The damage produced ahead of the crack tip through plastic deformation in the steel razor blade sharpened samples over against the lack of damage in the femtolaser sharpened specimens explains the disparity in the fracture values, as the crack tip radius was similar for all the test specimens. These differences reached values up to 11%, 75% and 90% when the crack growth initiation parameters were computed under LEFM, EPFM and PYFM conditions, respectively.

Acknowledgements

Authors are indebted to Ministerio de Educación of Spain for their financial support through projects MAT2006-13354 and MAT2009-14294, and to REPSOL YPF for the materials supply.

A. Segovia thanks the National Council of Science and Technology (CONACYT) of Mexico, for the support of a doctoral research scholarship.

References

[1] Williams JG. K_C and G_C at slow speeds for polymers. In: Moore DR, Pavan A, Williams JG, editors. Fracture mechanics testing methods for polymers, adhesives and composites. The Netherlands: Elsevier Science Ltd., and ESIS; 2001. p. 11–24.

[2] Hale GE, Ramsteiner F. J-fracture toughness of polymers at slow speed. In: Moore DR, Pavan A, Williams JG, editors. Fracture mechanics testing methods for polymers, adhesives and composites. The Netherlands: Elsevier Science Ltd., and ESIS; 2001. p. 123–57.

[3] Clutton E. Essential work of fracture. In: Moore DR, Pavan A, Williams JG, editors. Fracture mechanics testing methods for polymers, adhesives and composites. The Netherlands: Elsevier Science Ltd., and ESIS; 2001. p. 177–95.

[4] ASTM E1820-06: standard test method for measurement of fracture toughness; 2007.

[5] ASTM D5045-99: standard test methods for plane-strain fracture toughness and strain energy release rate of plastic materials; 1999.

[6] ASTM D6068-96: standard test method for determining *J–R* curves of plastic materials; 2002.

[7] Martínez AB, Segovia A, Gámez-Pérez J, Maspoch ML. Influence of femtolaser notch sharpening technique in the determination of essential work of fracture (EWF) parameters. Eng Fract Mech 2009;16:2604–17.

[8] Salazar A, Rodríguez J, Segovia A, Martínez AB. Influence of the notch sharpening technique on the fracture toughness of bulk ethylene–propylene block copolymers. Polym Test 2009. doi:10.1016/j.polymertesting.2009.09.004.

[9] Chichkov BN, Momma C, Nolte S, von Alvensleben F, Tünnermann A. Femtosecond, picosecond and nanosecond laser ablation of solids. Appl Phys A – Mater 1996;63:109–15.

[10] Moreno P, Méndez C, García A, Arias I, Roso L. Femtosecond laser ablation of carbon reinforced polymers. Appl Surf Sci 2006;252:4110–9.

[11] Pavan A. Determination of fracture toughness (G_{IC} and K_{IC}) at moderately high loading rates. In: Moore DR, Pavan A, Williams JG, editors. Fracture mechanics testing methods for polymers, adhesives and composites. The Netherlands: Elsevier Science Ltd., and ESIS; 2001. p. 27–58.

[12] Landes JD, Begley JA. The results from J-integral studies: an attempt to establish a J_{IC} testing procedure. Fract Mech ASTM STP 1974;560:170–86.

[13] Williams JG. Introduction to elastic–plastic fracture mechanics. In: Moore DR, Pavan A, Williams JG, editors. Fracture mechanics testing methods for polymers, adhesives and composites. The Netherlands: Elsevier Science Ltd., and ESIS; 2001. p. 119–22.

[14] Cotterell B, Reddel JK. The essential work of plane stress ductile fracture. Int J Fract 1977;13:267–77.

[15] Broberg KB. On stable crack growth. J Mech Phys Solids 1975;23:215–37.

[16] Hill R. On discontinuous plastic states with special reference to localized necking in thin sheets. J Mech Phys Solids 1952;1:19–30.

[17] Mai YW, Cotterell B, Horlyck R, Vigna G. The essential work of plane stress ductile fracture of linear polyethylenes. Polym Eng Sci 1987;27:804–9.

[18] Saleemi AS, Nairn JA. The plane-strain essential work of fracture as a measure of the fracture toughness of ductile polymers. Polym Eng Sci 1990;30(4):211–8.

[19] Levita G, Parisi L, Marchetti A. The work of fracture in semiductile polymers. J Mater Sci 1994;29(17):4545–53.

[20] Pardoen T, Marchal Y, Delannay F. Essential work of fracture compared to fracture mechanics – towards a thickness independent plane stress toughness. Eng Fract Mech 2002;69(5):617–31.

[21] Levita G, Parisi L, Mcloghlin S. Essential work of fracture in polymer films. J Mater Sci 1996;31:1545–53.

[22] Pardoen T, Marchal Y, Delannay F. Thickness dependence of cracking resistance in thin aluminum plates. J Mech Phys Solids 1999;47(10):2093–123.

[23] Brucato V, Piccarolo S, La Currabba V. An experimental methodology to study polymer crystallization under processing conditions. The influence of high cooling rates. Chem Eng Sci 2002;57:4129–43.

[24] Gamez-Pérez J, Santana O, Martínez AB, Maspoch ML. Use of extensometers on essential work of fracture (EWF) tests. Polym Test 2008;27:491–7.

[25] Gómez del Río T, Salazar A, Cea A, Hernández R, Rodríguez J. Temperature and strain rate on mechanical properties of ethylene–propylene block copolymers. Anales de Mecánica de la Fractura 2010:661–5.